Ciência Animal Brasileira
Brazilian Animal Science

DOI: 10.1590/1809-6891v25e-76225E

e-ISSN 1809-6891
Section: Veterinary Medicine | Research article

# 3D implant of copolyamide associated with thermoplastic elastomer (PCTPE) for tracheal repair in rabbits (*Oryctolagus cuniculus*): preliminary study

## Implante 3D de copoliamida associada à elastômero termoplástico (PCTPE) para reparação traqueal de coelhos (*Oryctolagus cuniculus*): estudo preliminar

**Ariadne Rein*[1], Marcelo Carrijo da Costa[1], Gabriel Montanhin[1], Gustavo Fernandes[1], Marcella Dall' Agnol Leite[1], Gabriel João Unger Carra[1],Rosemeri de Oliveira Vasconcelos[1],Luís Gustavo Gosuen Gonçalves Dias[1],Thiago André Salvitti de Sá Rocha[2],Paola Castro Moraes[1]**

1 Universidade Estadual Paulista (UNESP), Jaboticabal, São Paulo, Brazil
2 Universidade Federal de Jataí (UFJ), Jataí, Goiás, Brazil
*corresponding author: ariadne.rein@unesp.br

**Abstract:** Large segmental tracheal defects can pose a serious clinical challenge owing to the lack of suitable substitutes for reconstructive surgery. Polymeric biomaterials are widely used in medicine. However, the implantation of biomaterials triggers a series of biological events, and material biocompatibility is of paramount importance in regenerative medicine. The objective of this study was to evaluate the use of a copolyamide associated with thermoplastic elastomer (PCTPE) in 3D-printed prostheses for repairing partial tracheal defects in rabbits. Sixteen male New Zealand White rabbits were used, and partial tracheal defects were created in the ventral region from the 4th to the 8th tracheal ring. The animals were subdivided into groups (n=4) based on the time of euthanasia, scheduled at seven days (G7), 15 days (G15), 30 days (G30), and 60 days (G60). Histopathological analysis with hematoxylin and eosin staining revealed that the 3D implant of PCTPE exhibited a foreign body reaction, and inflammation persisted for up to 60 days. Histochemistry with picrosirius red revealed a tendency for a greater amount of type I collagen to accumulate in the early stages of inflammation, whereas type III collagen was predominant in later evaluation periods. These findings suggest an exacerbated and inadequate tissue-material interface reaction and perpetuation of the inflammatory process.

**Keywords**: bioprosthesis; picrosirius; polymers; regeneration; tracheoscopy

**Resumo:** Defeitos de grandes segmentos traqueais podem apresentar sério problema clínico, devido à ausência de substitutos na cirurgia reconstrutiva. Os biomateriais poliméricos

Received: May 25, 2023. Accepted: October 11, 2023. Published: January 15, 2024.

estão entre os mais utilizados na medicina. Entretanto, a implantação de um biomaterial desencadeia uma série de eventos biológicos e a biocompatibilidade do material é de extrema importância para a medicina regenerativa. Objetivou-se com este estudo avaliar o uso da copoliamida associada ao elastômero termoplástico (PCTPE) em próteses impressas em 3D para reparação de defeitos parciais da traqueia de coelhos. Foram utilizados 16 coelhos machos da raça Nova Zelândia Branco, submetidos à criação de um defeito parcial de traqueia na região ventral do 4º ao 8º anel traqueal. Os animais foram subdivididos (n=4) de acordo com o momento das eutanásias, programadas com intervalo de sete (G7), quinze (G15), trinta (G30) e sessenta dias (G60). A análise histopatológica por hematoxilina e eosina (HE) revelou que o implante 3D de PCTPE apresentou reação do tipo corpo estranho e a inflamação persistiu até os 60 dias de avaliação. A histoquímica de picrosirius vermelho revelou tendência de maior quantidade de colágeno tipo I nos tempos iniciais de inflamação, enquanto o colágeno tipo III foi predominante nos períodos tardios de avaliação. Pode-se sugerir reação exacerbada e não adequada da interface tecido-material e perpetuação do processo inflamatório.

**Palavras-chave:** bioprótese; picrosírius; polímeros; regeneração; traqueoscopia

## 1. Introduction

Large segmental tracheal defects pose a serious clinical challenge because of the absence of substitutes in reconstructive surgery. Tissue engineering is a promising approach for this issue[1]. The field of materials engineering is advancing, and biomaterials, whether of natural or synthetic origin, are substances that come into intimate contact with biological systems and can be part of the process of repairing or replacing a tissue or organ in the body for a certain period[2]. Polymers are widely used as biomaterials in the medical field. However, there is a need to develop new and more accessible biomaterials owing to the growing demand for personalized medical procedures[3].

One component currently under study is thermoplastic elastomer (TPE), which combines the elastic properties of rubber with the ease of processing at high temperatures[4]. A copolymer associated with TPE (PCPTE) was produced to combine the flexibility of TPE with the durability of nylon[5]. 3D printing creates objects by layering materials (FDM) based on a virtual model generated by a computer from segmented two-dimensional cross-sectional data, allowing for precise and cost-effective model production in a short time[6].

This study aimed to evaluate the use of a custom 3D-printed implant with a copolymer associated with TPE for the repair of partial tracheal defects in rabbits.

## 2. Materials and methods

This study followed the ethical standards and principles of animal experimentation approved by the National Council for the Control of Animal Experimentation (CONCEA) and Ethics Committee for Animal Use (CEUA) (approval no. 006161/19). Sixteen healthy male New Zealand White rabbits (*Oryctolagus cuniculus*) weighing between 3 and 3.5 kg and aged 7

months were obtained from the Central Animal Facility of the Faculty of Veterinary Medicine and Animal Science, UNESP, Botucatu Campus, Brazil. The animals were divided into four groups based on the following postoperative evaluation times: seven days (G7), 15 days (G15), 30 days (G30), and 60 days (G60), with four animals in each group (n=4). The material used was a copolyamide associated with TPE (PCPTE), manufactured by Taulman 3D, LLD, in the form of a white 1.75-mm monofilament for 3D printing.

The prosthesis was designed using SolidWorks 2016 three-dimensional prototyping software and printed using the fused deposition modeling method on a Prusa model 13 printer. The dimensions were based on the average obtained in a pilot study conducted by the research group using an ex vivo model of rabbit trachea, with the following dimensions: 4 mm cranial circumference diameter, 5 mm caudal circumference diameter, and 0.5 mm wall thickness. The prototypes were produced by VetCraft®, packaged in surgical-grade paper, and autoclaved in a rapid cycle at 121°C for 15 min. At the time of surgery, the implant was cut in half using Mayo scissors (Figure 1).

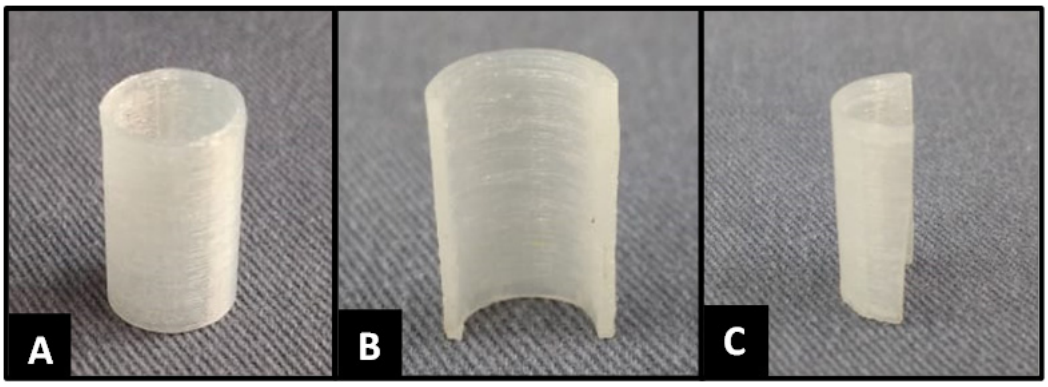


**Figure 1 3D-printed implant for repairing partial tracheal defects in rabbits using the fused deposition modeling method with PCTPE material. (A) Implant immediately after printing (circular shape); (B) view of the inner part; and (C) lateral view of the finished implant.**

## 2.1 Anesthetic protocol and surgical procedure

The animals were anesthetized with chlorpromazine hydrochloride (Longactil®, Cristália Indústria Farmacêutica, São Paulo, Brazil) at a dose of 0.5 mg/kg and morphine (Dimorf®, Cristália Indústria Farmacêutica, São Paulo, Brazil) at a dose of 0.5 mg/kg, both administered intramuscularly. Anesthetic induction was performed with propofol (Propovan®, Cristália Indústria Farmacêutica, São Paulo, Brazil) at a dose of 10 mg/kg administered intravenously, followed by orotracheal intubation using a size 3.0 endotracheal tube. Inhalation anesthesia was maintained using isoflurane (Isoforine®, Cristália Indústria Farmacêutica, São Paulo, Brazil) diluted in 100% oxygen through an anesthesia machine with a total flow rate of 1 L/min.

The procedure was performed following all principles of aseptic surgery, with surgical instruments, sterile gauze, dressings, and surgical drapes. The surgical team remained the same across all groups. The surgical field was prepared by performing extensive trichotomy (hair removal) from the ventral cervical region to the manubrium. Subsequently, both

preoperative and postoperative antiseptic procedures used a 2% chlorhexidine germicidal solution followed by 70% alcohol.

A skin incision was made along the midline of the ventral cervical region, immediately caudal to the cricoid cartilage and extended down to the manubrium. Subsequently, a subcutaneous dissection was performed, and the sternohyoid muscles were located and retracted to expose the trachea. Delicate dissection was performed only in the area to be manipulated to avoid damaging the innervation of the site. A defect was created in the ventral region of the trachea using a no. 15 scalpel blade. The cartilaginous rings were incised from the fourth to the eighth tracheal rings, with an extension equivalent to five tracheal rings, resulting in a partial ventral defect of full thickness that exposed the tracheal lumen.

After creating the tracheal defect, the previously custom-made PCTPE material implant, 3D-printed, was fixed beneath the defect to cover it with 4-0 polypropylene sutures. Initially, the suture thread was passed through the trachea and prosthesis, anchored with hemostatic forceps, and the knots were tied alternately for better distribution of suture forces (Figure 2). Although the PCTPE prosthesis was rigid, passage of the suture needle was possible. Subsequently, the sternohyoid muscles were repositioned, the subcutaneous tissue was approximated using a zigzag suture pattern, and the skin was sutured using a separate simple suture pattern with 3-0 nylon thread.

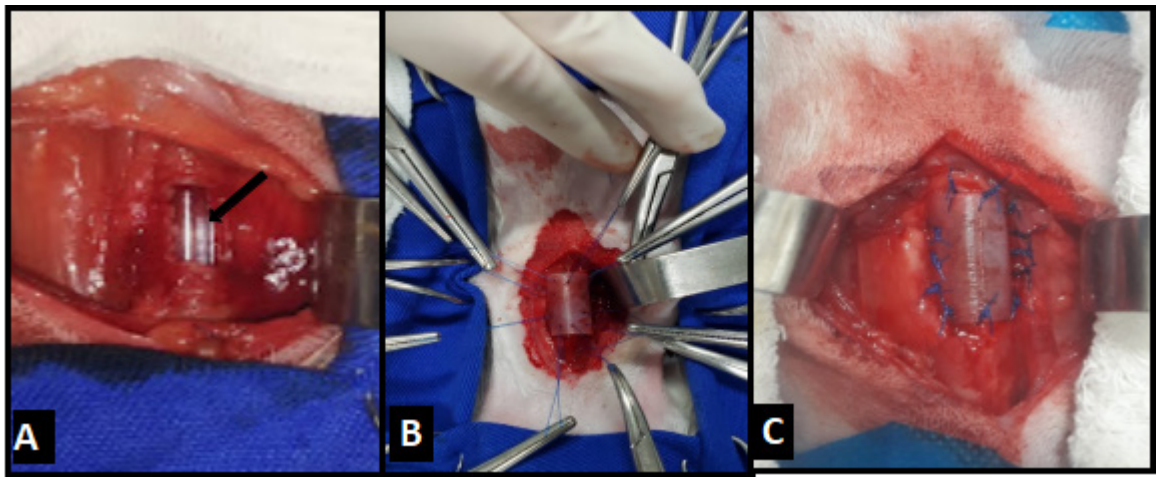


**Figure 2 (A) Partial tracheal defect in rabbits created between the 4th and 8th tracheal ring, with the endotracheal tube indicated by the black arrow; (B) Anchoring of suture points of the PCTPE implant on the trachea; (C) Completed suturing of the PCTPE implant covering the tracheal defect.**

## 2.2 Postoperative evaluation

In the immediate postoperative period, the animals were administered hydrocortisone (Cortisonal®, União Química Nacional S/A, São Paulo, Brazil) at a dose of 50 mg/kg intravenously (single application); tramadol hydrochloride (Tramadon®, Cristália Indústria Farmacêutica, São Paulo, Brazil) at a dose of 4 mg/kg intramuscularly, and enrofloxacin (Chemitril®, Chemitec Agro-Veterinária, São Paulo, Brazil) at a dose of 5 mg/kg subcutaneously. They

were monitored and kept warm until they regained consciousness and exhibited normal respiratory patterns.

Antimicrobial therapy with enrofloxacin and analgesia with tramadol hydrochloride were maintained at the same doses and routes of administration mentioned earlier for five consecutive days, with a 12-h interval between doses. Throughout the evaluation period, the rabbits were kept in individual cages suitable for their species, with access to water and commercial food, and the environment was temperature-controlled.

The animals were evaluated daily for respiratory patterns, respiratory noises, the presence or absence of wound secretions, subcutaneous emphysema, and overall behavior. Excessive handling was avoided to prevent stress and the potential development of dyspnea. Euthanasia was performed in the respective groups at the following time intervals: 7, 15, 30, and 60 days after surgical intervention. The euthanasia method adhered to the ethical principles of animal experimentation established by CONCEA. This was carried out by intravenous administration of propofol (dose effect), and once the absence of corneal and pupillary reflexes was confirmed, 20 ml of potassium chloride was administered intravenously to induce asystole.

### 2.3 Tracheoscopy

Tracheoscopy was conducted immediately following euthanasia using a rigid 4-mm, 30-degree endoscope (Karl Storz-endoskope®, Telecam SL NTSC® microcamera, Hopkins II® optics with a 250 Twin® cold halogen light source and Xênon 100®).

Additionally, tracheoscopy was performed on four anesthetized rabbits for other experimental procedures by the same team without any surgical intervention or orotracheal intubation, with the aim of obtaining images for comparison with normal rabbit trachea. The internal surface of the implant was evaluated for the presence of secretions and intraluminal granulomas. These findings were graded by two non-blinded assessors using the following scores: absent (0), mild (1), moderate (2), and severe (3). The visibility of suture points and prosthesis coverage by tissue was characterized as either "yes" or "no." The grading of tracheal lumen narrowing was adapted from the tracheal collapse classification in dogs proposed by Tappin[7] and included absent (0), grade I: 25% reduction of the lumen (1), grade II: 50% reduction of the lumen (2), grade III: 75% reduction of the lumen (3), and grade IV: total loss of the lumen (4).

### 2.4 Macroscopic evaluation after euthanasia

The surgical site was assessed after euthanasia for the following: signs suggestive of inflammation or foreign body reaction based on tissue discoloration, increased volume at the surgical site, and content or secretion upon cutting. The assessment parameters were graded as absent (0), mild (1), moderate (2), or severe (3).

### 2.5 Histological evaluation

The tissue samples were processed according to standard histological processing protocols, including embedding in paraffin blocks and preparation of histological sections. The sections were cut using a microtome with a thickness of 4 µm. After creating slides, specific staining was performed using hematoxylin and eosin (HE) and Masson's trichrome. Owing to the rigidity of the implant, it was necessary to remove it before sectioning, and the implant-trachea interface area was analyzed. Histological analysis of the sections was conducted by an experienced pathologist who was blinded to group identities. Histological slides were evaluated under an optical microscope. Photomicrographs were obtained using the Olympus Cell Sens Standard software 1.18. The data obtained for epithelialization, fibrosis, inflammation, capillaries, and cartilaginous tissue were classified according to the intensity in which they were found and transformed into semi-quantitative variables by assigning an index for histological findings, following the criteria of Jung et al.[8]. The presence of goblet cells in the tracheal epithelium was assessed by two evaluators and scored as follows: - (absent); + (mild increase); ++ (moderate increase); +++ (severe increase); R0 (no reduction); R1 (mild reduction); R2 (moderate reduction); R3 (severe reduction).

The histochemical staining with picrosirius red was performed following the instructions of the commercial kit Picrosirius Histokit® from EasyPath Diagnósticos. The evaluation was then conducted using an optical microscope with polarized light, specifically a Nikon® ECLIPSE E200 microscope equipped with a Tucsen® HD Lite camera and Tucsen® TCapture 5.1.1 software. Photomicrographs of three fields within the area of interest were captured using a 20X objective. The measurement of the area of collagen type I and collagen type III was performed with ImageJ® software using the Threshold Color plugin, as suggested by Bedoya et al.[9] based on standardized color ranges. For green (collagen type III), the color parameters were set to 45-120, and for red (collagen type I), the color parameters were set to 0-40 and 190-255. The saturation parameter was maintained at 0-255, and the brightness parameter was automatically established by the software.

### 2.6 Statistical analysis

The variables related to clinical evaluation, tracheoscopy, and postmortem macroscopy were subjected to the chi-square test and confirmed using Fisher's exact test at a 5% significance level. Statistical analyses were conducted using Statistical Analysis Software (SAS version 9.3, SAS Institute, Cary, NC, USA). Histological data from HE staining and collagen quantification using picrosirius red were subjected to the Pearson test and confirmed by the Kruskal-Wallis test at a 5% significance level. These analyses were performed using R version 4.3.0.

## 3. Results and discussion

Of the 16 operated animals, one succumbed to the condition 12 days after the surgical procedure. This animal was assigned to the 60-day group. It presented with severe dyspnea, cyanosis of the oral mucosa, and orthopneic position, and progression of the condition

occurred within a single day. Although there was no increase in volume at the surgical site, there was a significant amount of serous secretion in the tracheal lumen. Tracheal stenosis and intraluminal granuloma formation were not observed during the postmortem evaluation. This animal was excluded from the statistical analyses.

### 3.1 Clinical evaluation

None of the animals exhibited emphysema, seroma, or wound secretions. Anorexia, other gastrointestinal changes, and behavioral alterations were not observed. Throughout the evaluation period, the animals remained active and did not exhibit any significant respiratory pattern alterations. No significant weight loss was observed before the experiment or before euthanasia in each group (Table 1).

According to Grillo[10], the prerequisites for successful tracheal reconstruction include the substitute having rigidity and allowing air passage without causing collapse, as well as flexibility to permit neck movement without implant fracture. The PCTPE prosthesis exhibited these characteristics, as no animal experienced tracheal rupture, and they maintained normal neck movement, which was observed in their behavior within the cage, during feeding, and while drinking water throughout the 60-day evaluation period.

**Table 1 Weight of rabbits undergoing partial tracheal defect reconstruction with a 3D PCTPE prosthesis at the time of surgery and euthanasia**

| Group | | Weight (kg) | |
|---|---|---|---|
| | Animal | Surgery | Euthanasia |
| 7 days | 1 | 3.5 | 3.4 |
| | 2 | 3.4 | 3.3 |
| | 3 | 4.4 | 4.4 |
| | 4 | 4.6 | 4.6 |
| 15 days | 1 | 3.8 | 4.0 |
| | 2 | 4.2 | 4.4 |
| | 3 | 3.7 | 3.5 |
| | 4 | 3.5 | 3.2 |
| 30 days | 1 | 3.4 | 3.6 |
| | 2 | 3.8 | 3.8 |
| | 3 | 3.6 | 4.0 |
| | 4 | 3.7 | 4.2 |
| 60 days | 1 | 4.2 | 4.0 |
| | 2 | 3.7 | 4.0 |
| | 3 | 3.5 | 3.7 |

### 3.2 Tracheoscopy

The tracheoscopic findings did not show any significant differences between the groups. The intraluminal secretion observed during tracheoscopy had similar characteristics in all animals: a yellowish, thick secretion adhering to the prosthesis or tracheal wall, with variations in quantity and distribution (Figure 3). The second crucial prerequisite for successful long-term

tracheal replacement is the presence of specialized respiratory epithelium that serves as a barrier against infections and expels foreign bodies[10, 11].

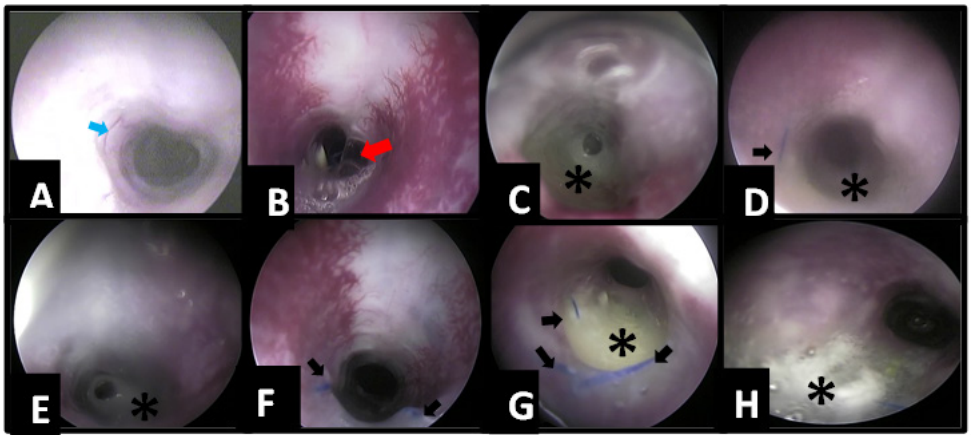


**Figure 3 Tracheoscopy of rabbits with partial tracheal defect reconstruction using a 3D PCTPE implant. (A) and (B) 7 days. (A) Absence of secretion at the implant site, visualization of tissue covering the prosthesis, blood vessel (blue arrow). (B) Presence of intertwined suture in the center of the prosthesis (red arrow), tracheal stenosis grade I - 25% reduction in lumen. (C) and (D) 15 days. (C) Moderate secretion present at the implant site (*), irregular surface. (D) Mild secretion present at the implant site (*), suture thread visible (black arrow). (E) and (F) 30 days. (E) Significant secretion at the implant site (*). (F) Absence of secretion at the implant site, suture thread visible (black arrows). (G) and (H) 60 days. (G) Moderate secretion at the implant site (*), suture thread visible (black arrows).**

The visibility of the tissue covering the prosthesis and suture points during tracheoscopy is a positive indicator of the interaction of the biomaterial with the host as well as the absence of intraluminal granulomas. This suggests that the biomaterial is well tolerated by the host and that the healing process is progressing favorably without the formation of abnormal tissue masses within the tracheal lumen.

A study by Jung et al.[8] that assessed ciliary beat frequency as an important indicator of specialized respiratory epithelial function in rabbits undergoing partial tracheal defect reconstruction with a 3D polyurethane prosthesis provided valuable insights. They observed the presence of ciliary beat frequency starting at eight weeks post implantation of the prosthesis, which was the same maximum evaluation timeframe as in our study. This suggests the gradual recovery of specialized respiratory epithelial function.

### 3.3 Macroscopic post-mortem evaluation

Macroscopic findings of direct inspection of the surgical site after euthanasia, such as volume increase and secretion upon cutting, did not show any significant time-dependent differences. During access to the collected tracheal material, some animals exhibited yellow, thick, and localized secretion beneath the skin at the surgical site, suggesting abscess formation (Figure 4). In the G7 group, none of the animals displayed an increase in volume at the wound site. In G15, two animals showed a slight increase in volume (25%), and one showed a moderate increase in volume (25%) with a moderate amount of yellow secretion

upon cutting. In the G30 group, two animals showed a slight increase in volume (50%), and one animal displayed a moderate increase in volume (25%), with a moderate amount of yellow secretion upon cutting. In the G60 group, only one animal showed a slight increase in volume with a moderate amount of secretion upon cutting (25%). Changes in tissue color at the surgical site were absent in all animals in all groups. According to Townsend et al.[12], direct contact of air with the implant in the trachea allows for colonization by various bacteria.

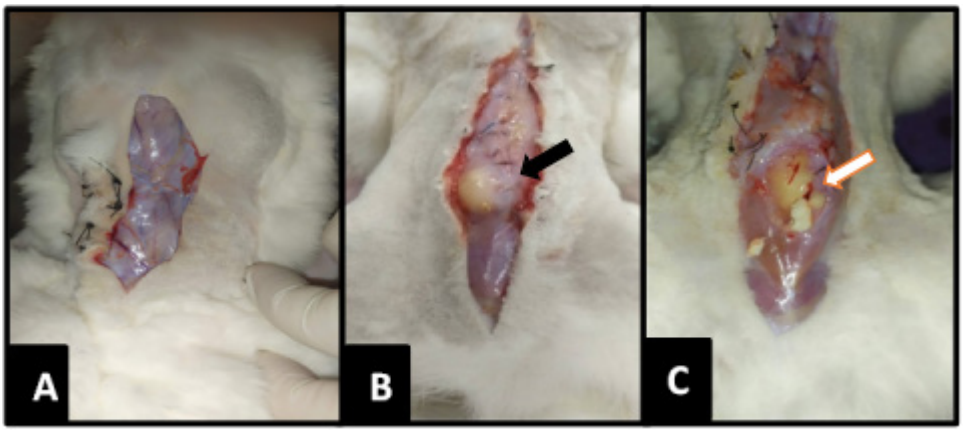


**Figure 4 Macroscopic evaluation of the trachea after euthanasia of rabbits. (A) Rabbit from the G15 group with no increase in volume and no secretion at the surgical site; (B) and (C) another rabbit from the G15 group with a moderate increase in volume at the surgical site (black arrow), after skin incision, a circumscribed area with a yellowish color is observed; upon incision of the muscle suture, yellowish secretion is present (white arrow).**

No bacterial cultures were performed from the surgical wound; however, the loss of tracheal integrity associated with the synthetic prosthesis predisposed the animal to opportunistic infections of the respiratory tract, and the perpetuation of the infection prevented or delayed the re-epithelialization of the trachea, which was also present in the tracheal lumen by tracheoscopy. As an alternative, Kang et al.[13] used tissue engineering to associate a fibrous membrane with antimicrobial properties to the scaffold to replace the trachea, previously tested for *E. coli* and *Staphylococcus* sp., and concluded that the presence of the antimicrobial membrane accelerated the re-epithelialization of the trachea. The omentum can also be used as an alternative to avoid infection and accelerate re-epithelialization of the trachea, as reported with positive results by other authors using pedicled flaps and culture of the scaffold in an *in vivo* bioreactor[14].

### 3.4 Histological evaluation

The first generation of biomaterials was developed to be bioinert, with the primary goal of preventing foreign body reactions[15]. However, implantation of a biomaterial triggers a series of biological events[16]. According to Williams[17], some of the main expected reactions of a biomaterial in its host include neutrophil activation, macrophage activation, production of foreign body giant cells, granulation tissue formation, fibrosis, microvascular changes, specific tissue responses (e.g., osteoclasts and osteoblasts for bone), and endothelial proliferation.

In the present study, the tissue reaction to the 3D PCTPE implant in the trachea was evident. Histological findings in the interface-implant region included epithelialization, inflammatory infiltration in the basal membrane and epithelium, the presence of fibrous tissue, an increase or decrease in goblet cells, neovascularization in the submucosa, and an increase in the volume of the tracheal ring cartilage, characterized by an increase in the number of chondrocytes in the tracheal rings (Figure 5). Catarrhal and mucopurulent exudates were observed in the lumen. Changes in the epithelium correspond to the transition from pseudostratified to stratified epithelium. The distribution of results by group is presented in Table 2.

Inflammation was not significantly different between the groups, and the presence of inflammatory infiltrates in the region of the epithelium and the basal layer of the implant-trachea interface area was identified in all groups up to 60 days of evaluation. This biomaterial is expected to trigger a sterile inflammatory response, resulting in a balance between inflammation and fibrosis[18]. In biocompatible materials, the chronic inflammatory response, characterized by the presence of mononuclear cells, lasts for a maximum of two weeks. The persistence of acute inflammation or inflammatory responses beyond the three-week period generally indicates infection[16].

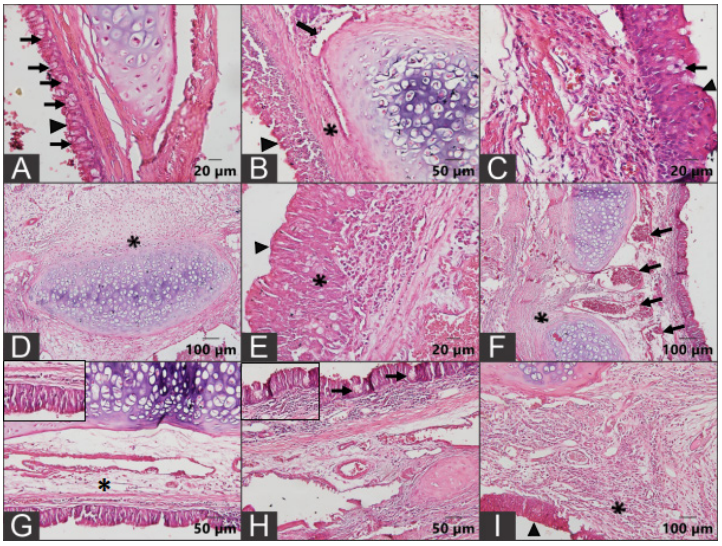


**Figure 5 Photomicrographs of the rabbit trachea with partial defect reconstruction using a 3D PCTPE prosthesis. (A) Normal tracheal region with pseudostratified columnar ciliated epithelium (arrowhead), presence of goblet cells (black arrows) (scale bar = 20 µm); (B) G7 animal, stratified columnar epithelium (arrowhead), fibrosis in the submucosa (*), and tracheal cartilage hyperplasia with the presence of chondroblasts (black arrow) (scale bar = 50 µm); (C) G7 animal, stratified ciliated columnar epithelium (arrowhead), goblet cells (black arrow) (scale bar = 20 µm); (D) G15 animal, tracheal cartilage hyperplasia with the presence of chondroblasts (*) (scale bar = 100 µm); (E) G15 animal, stratified squamous columnar epithelium, absence of cilia (arrowhead), fibrosis (), (scale bar = 20 µm); (F) G30 animal, stratified ciliated columnar epithelium (arrowhead), submucosa without fibrosis and with a large number of blood vessels (black arrows) (scale bar = 100 µm); (G) and (H) G60 animal, (G) stratified columnar epithelium with the presence of cilia (highlighted in the upper left corner), submucosa without fibrosis with discrete mononuclear inflammatory infiltrate () and (H) showing the presence of goblet cells in clusters in the epithelial region (black arrows, highlighted in the upper left corner) (scale bar = 50 µm); (I) G60 animal, stratified columnar epithelium, absence of cilia (arrowhead), mononuclear inflammatory infiltrate in the submucosa (*) (scale bar = 100 µm); Hematoxylin and eosin.**

The presence of pyogranulomas, phlegmon, and necrosis in the adjacent muscle tissue in the region of interest was also observed in three animals of G7 (75%), one animal of G15 (25%), two animals of G30 (50%), and two animals of G60 (67%) (Figure 6). According to Gaissert et al.[19], the inflammatory process induced by synthetic tracheal prostheses can favor the presence of infectious processes in adjacent tissues.

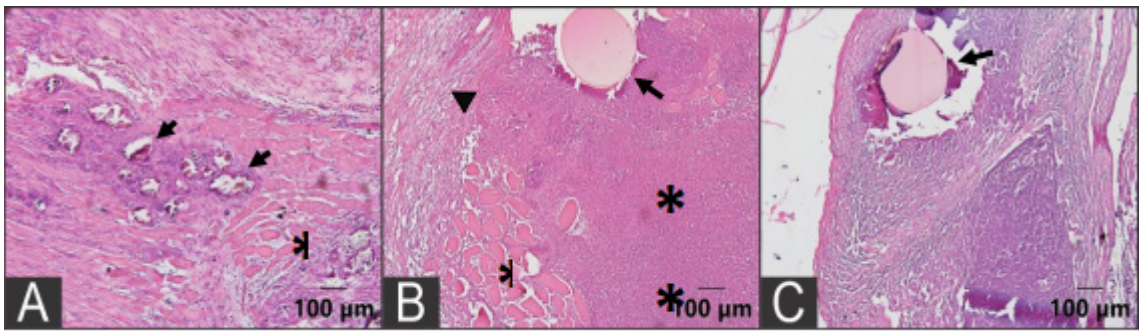


**Figure 6 Photomicrographs of skeletal muscle from the region adjacent to the 3D PCTPE prosthesis used to cover partial tracheal defects in rabbits. (A) An animal from G7 showing skeletal muscles with coagulative necrosis (*) and areas of dystrophic calcification (black arrows) (scale bar = 100 µm). (B) An animal from G15 with skeletal muscle exhibiting coagulative necrosis () and an extensive area of liquefactive necrosis (**) (abscess) around an amorphous acidophilic structure (suture thread). Adjacent to this area, fibrosis is observed (arrowhead, scale bar = 100 µm). (C) An animal from G30 showing the presence of a pyogranuloma around an amorphous acidophilic structure (suture thread, black arrow) (scale bar = 100 µm). Hematoxylin and eosin.**

**Table 2 Summary of macroscopy, laryngoscopy, and microscopy (HE) results for groups G7, G15, G30, and G60 of rabbits undergoing partial tracheal defect reconstruction with 3D PCTPE prosthesis**

| Animal group | | Macroscopy | | Laryngoscopy | | Microscopy (HE) | | | | | | |
|---|---|---|---|---|---|---|---|---|---|---|---|---|
| | | Increase in tissue volume | Secretion upon cutting | Secretion in the lumen | Narrowing | Epithelialization | Inflammation | Fibrosis | Goblet cells | Presence of exudate | Epithelial Type | Angiogenesis |
| 7 days | 1 | - | - | + | 0 | ++ | ++ | +++ | R0 | ++ | PSE | +++ |
| | 2 | - | - | - | 0 | +++ | + | ++ | R3 | - | E | ++ |
| | 3 | - | - | - | 0 | +++ | +++ | + | R2 | + | E* | + |
| | 4 | - | - | + | 1 | ++ | + | + | R1 | + | E | ++ |
| 15 days | 1 | - | - | ++ | 0 | ++ | ++ | + | ++ | + | E | + |
| | 2 | ++ | ++ | + | 0 | ++ | ++ | + | +++ | - | E | +++ |
| | 3 | + | - | + | 0 | +++ | ++ | ++ | R2 | - | E | ++ |
| | 4 | - | - | + | 0 | ++ | +++ | ++ | R1 | + | E | ++ |
| 30 days | 1 | ++ | ++ | +++ | 2 | ++ | ++ | ++ | +++ | ++ | E | ++ |
| | 2 | + | - | - | 2 | ++ | + | + | ++ | + | E | + |
| | 3 | - | - | + | 0 | + | + | + | ++ | + | E | ++ |
| | 4 | - | - | - | 0 | + | + | + | R1 | - | E* | ++ |

| | | | | | | | | | | | | |
|---|---|---|---|---|---|---|---|---|---|---|---|---|
| 60 days | 1 | - | - | - | 0 | + | ++ | + | R1 | - | E | + |
| | 2 | - | - | ++ | 0 | + | + | + | R0 | - | E | ++ |
| | 3 | + | ++ | ++ | 0 | + | + | ++ | R2 | - | E* | ++ |

*-: absent; +: discreet; ++: moderate; +++: marked;*
*0: no alteration; 1: grade I (25% reduction in lumen); 2: grade II (50% reduction in lumen); 3: grade III (75% reduction in lumen); R0: no reduction; R1: slight reduction; R2: moderate reduction; R3: marked reduction.*
*HE: hematoxylin and eosin; PSE: pseudostratified ciliated columnar; E: stratified squamous columnar; *: presence of cilia.*

The trachea is composed of different tissues, including the epithelial layer, submucosa, hyaline cartilage, and segmental vascularization, which makes its reconstruction challenging. Additionally, in the respiratory tract, inspired air carries bacterial contamination and can disrupt the anastomosis of the implant with the tracheal tissue, which may hinder the growth of the respiratory epithelium. PCTPE is a rigid material, and although the animals did not develop subcutaneous emphysema, it was not possible to completely seal the organ, thus allowing a small amount of air to pass into the adjacent tissues. This could explain the changes observed in the muscular tissues.Neovascularization in the submucosa was evident at all time points. Rich vascular support is important for cartilage regeneration. The repair response of the cartilage was observed at all evaluation time points, with the presence of young cells at the periphery of the cartilage. This is consistent with the findings of Chang et al.[22], who used a 3D-printed polycaprolactone scaffold coated with mesenchymal cells seeded in fibrin. Han et al. [23] reported the use of mesenchymal stem cells associated with biomaterial scaffolds for the regeneration of various tissues, including the trachea, as a promising approach in tissue engineering.

After tissue damage, the tissue repair process begins, which consists of a sequence of cellular, molecular, and biochemical events aimed at restoring the integrity of the injured tissue [24]. Tissue repair is a complex process divided into stages with somewhat indistinct boundaries that overlap over time. These stages include hemostasis, the inflammatory phase, formation of granulation tissue with the deposition of extracellular matrix (collagen, elastin, and reticular fibers), and remodeling [25,26, 27].

In picrosirius red staining, thicker type I collagen fibers are expressed in a red/orange color, whereas thinner mature collagen fibers are expressed in green. This differential staining allowed the quantitative evaluation of collagen types I and III[28]. The expression of collagen types I and III did not show significant differences between the groups ($p > 0.05$) according to the Kruskal-Wallis test, which was confirmed by the Dunn test. However, there was a tendency for decreased expression of collagen type I in the groups with longer incubation times (G30 and G60) compared to that in the group with a shorter time (G7), with the lowest expression in G60. Conversely, collagen type III expression increased with time, with the highest expression in G60, as shown in the graph (Figure 7). These data are consistent with the findings of Varghese et al.[29], who observed that fibroinflammatory hyperplasia exhibits intense red-orange polarization.

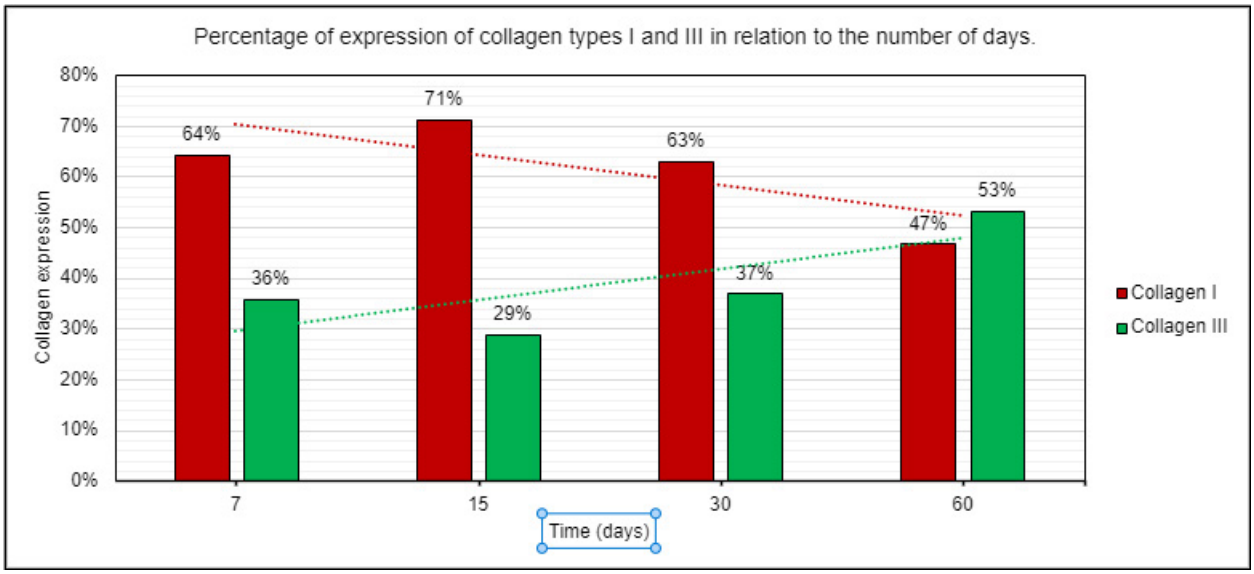


**Figure 7 Bar chart with trend line showing the percentage of expression of type I and type III collagen fibers in relation to time in days in rabbits undergoing partial tracheal defect repair with 3D PCTPE prosthesis.**

Granulation tissue is formed three four days after the injury[30]. This justifies the higher number of type I collagen fibers in the early evaluation periods, consistent with the initial inflammatory phase. The presence of type III collagen fibers refers to loose connective tissue fibers, which can be composed of pro-collagen, intermediate collagens, and pathological collagens[31]. Morales et al.[32] reported higher levels of type III collagen in patients with pulmonary fibrosis.

Reis et al.[33] and Jahshan et al.[34] showed that tracheal stenotic lesions induced by orotracheal intubation in humans and rats, respectively, had increased tracheal tissue fibrosis, which was quantitatively evaluated using the histochemical technique of picrosirius red staining. Reis et al.[33] observed a higher expression of type I collagen in the control group of human tracheas, with variation according to the evaluation site, more intense expression near the glands and blood vessels, and less intense expression in areas with loose connective tissue. The group with stenotic trachea, showing submucosal hypertrophy and hyperplasia and areas of squamous metaplasia in the tracheal epithelium, had higher expression of type I collagen, without distinction between the epithelial and basal layers. This finding is consistent with the present study, where a moderate positive correlation ($r=0.55$) was observed, with a significance above 95% ($p=0.02$), between the type I collagen index and the epithelialization index.

The respiratory epithelium of the trachea has a great proliferative capacity and is capable of continuous renewal above the basal membrane after injury, as long as the stem cells have not been destroyed. If tissue damage involves the epithelial and submucosal layers, regeneration does not occur independently. In such situations, the repair process occurs through the deposition of collagen fibers, forming a scar. Therapies for tracheal repair should aim for regeneration while avoiding scar formation[20] to maintain organ function.

However, unlike Reis et al.[33], whose study of the normal trachea showed a higher incidence of type I collagen at 60 days with the PCTPE prosthesis, we found a higher expression of type III collagen. Although G60 showed a smaller amount of fibrous tissue in the basal membrane compared to the other groups as assessed by HE and Masson's trichrome staining (Figure 8), the persistence of inflammation until G60 may have delayed collagen maturation.

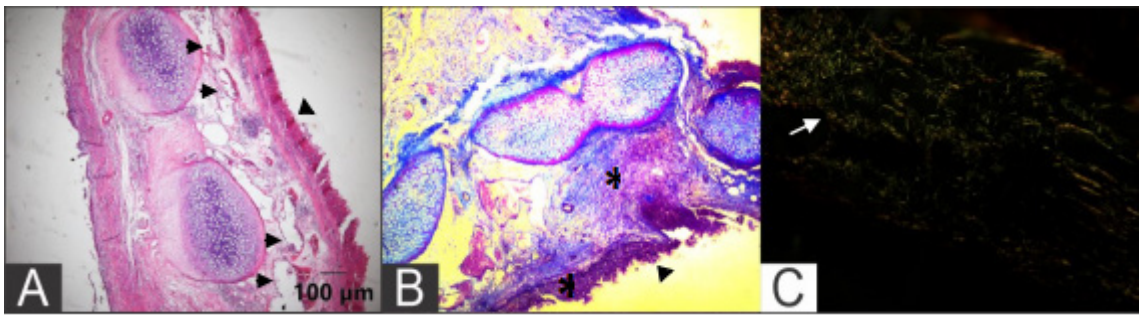


**Figure 8 Photomicrographs of the rabbit trachea after partial defect reconstruction with a PCTPE 3D prosthesis, implant-trachea interface region of G60. (A) In the HE staining, note the presence of proliferating chondrocyte cells at the periphery of the tracheal ring (*), along with marked neovascularization in the submucosa (black arrows) and the presence of stratified columnar epithelium lining the mucosa (arrowhead) (Scale bar = 100 µm); (B) In Masson's trichrome staining, there is a small amount of mature collagen in the submucosa, with disorganized fibers (loose connective tissue) (). The mucosa epithelium is stratified columnar (arrowhead) (10x objective). (C) Picrosirius red histochemical method under polarized light, showing a predominance of collagen type III fibers (green, white arrow) (20x objective). HE, hematoxylin and eosin.**

Synthetic models developed for tracheal replacement offer advantages, such as adaptation to the predetermined shape, size, and biomechanical characteristics; however, they have shortcomings, as they do not acquire the macro- and micro-anatomical structures of the organ[22,35]. The tracheal epithelium is pseudostratified and columnar, with cilia and goblet cells that produce mucus. The beating of cilia toward the larynx transports particles and cellular debris from the lungs and expels them from the body[36]. Decreases and increases in goblet cells in the epithelium of the implant-trachea interface region were observed, along with the presence of exudate in the tracheal lumen.

Garcia et al.[37] identified goblet cells as possible precursors of multiciliated cells because of the presence of hybrid cells that coexpressed markers of both goblet and multiciliated cells. The presence of goblet cells in the implant-trachea interface region may partly suggest regeneration of the epithelium in that area. However, even if cilia were observed in one animal from G60 with an unaltered submucosal layer, this does not necessarily mean that their movement is adequate and functional. This could explain the presence of secretions in the prosthesis region visualized during tracheoscopy at all evaluation periods. Measuring ciliary beat frequency would be the most appropriate assessment for epithelial functionality, as performed by Jung et al.[8], and is one of the limitations of the current study.

Biomaterials are not essential to regenerative medicine. Regenerative medicine includes therapies that induce tissue or organ regeneration, which can be achieved through gene

therapy, cell therapy, or tissue engineering. In this context, biological materials serve as adjuncts, making their biocompatibility crucial[17]. The present study evaluated the use of the PCTPE polymer and its reactions in the rabbit trachea without the intervention of any adjuvant therapy. It was possible to observe that foreign body reactions were evident at all time points, causing changes in the epithelium, submucosa, and cartilage in the area of interest, but without generating significant clinical changes up to 60 days of evaluation.

Fused deposition modeling (FDM) is the most common and cost-effective type of additive manufacturing technology. In medicine, FDM is used to manufacture customized patient-specific devices such as implants, prostheses, anatomical models, and surgical guides[2]. The FDM 3D printing method has proven to be effective in creating a customized tracheal prosthesis with desired characteristics, such as the shape to cover a partial defect in the rabbit trachea.

Alternative methods of managing tracheal defects have been studied for many years[38]. Polymers have a wide range of applications and are used in various medical fields. A biocompatible polymer promotes function without altering homeostasis or causing allergies or other side effects[39]. Further studies are needed to assess the biocompatibility of PCTPE in the trachea, as well as the development of new biomaterials that can be combined with regenerative medicine techniques for improved results.

The limitations of this study include the performance of tracheoscopy only immediately post-mortem, which did not reveal the evolution of each individual during the analysis period, and the small number of animals per group (n=4), which may have contributed to the lack of statistically significant differences in the applied analyses. This study did not propose a biocompatibility analysis, as it would require additional evaluations, such as chemical and toxicity assessments. This was a preliminary study of the interaction between PCTPE material and tracheal tissue.

## 4. Conclusion

The 3D-printed PCTPE prosthesis showed a prolonged inflammatory response lasting up to 60 days, which suggests an exaggerated and inadequate tissue-material interface reaction. However, it should be considered, as previously reported by other authors, that the main challenge in using synthetic prostheses in the trachea is the regeneration of specialized epithelium that prevents respiratory tract infections, which is essential for long-term success. Therefore, we cannot claim that the functionality of the respiratory epithelium was fully restored. With advancements in regenerative medicine, further studies involving PCTPE in the trachea should be conducted, as the use of adjuvants may provide better results, as described in the literature with other biomaterials.

### Declaration of conflict of interest

The authors declare that there is no conflict of interest.

## Author contributions

*Conceptualization*: A. Rein, M.C. da Costa and P.C. Moraes. *Formal analysis*: G.J.U Carra. *Investigation*: A. Rein, M.C. da Costa, G. Fernandes, G.L. Montanhim, M.D. Leite and R.O. Vasconcelos. *Methodology*: A. Rein, M.C. da Costa, P.C. Moraes and T.S.S. Rocha. *Project administration*: A. Rein and P.C. Moraes. *Supervision*: P.C. Moraes and L.G.G. Dias. *Writing (original draft)*: A. Rein. *Writing (review and editing)*: A. Rein and P.C. Moraes.

## Acknowledgments

This study was funded by the Coordenação de Aperfeiçoamento de Pessoal de Nível Superior (CAPES) with support from the Conselho Nacional de Desenvolvimento Científico e Tecnológico- CNPq-Brasil.

## References

1. Gao B, Jing H, Gao M, Wang S, Fu W, Zhang X, He X, Zheng J. Long segmental tracheal reconstruction in rabbits with peddicled Tissue-engineered trachea based on a 3D printed scaffold. Acta Biomaterialia. 2019; 97(1):177–186. https://doi.org/10.1016/j.actbio.2019.07.043

2. Tappa, K., e Jammalamadaka, U. (2018) Novel biomaterials used in medical 3D printing techniques. Journal of Functional Biomaterials, 9(1). https://doi.org/10.3390/jfb9010017

3. Pires ALR, Bierhals ACK, Moraes AM. Biomateriais: tipos, aplicações e mercado. Química Nova. 2015; 38(7):957–971. https://doi.org/10.5935/0100-4042.20150094

4. De Risi FR, Noordermeer JWM. Effect of Methacrylate Co-Agents on Peroxide Cured PP/EPDM Thermoplastic Vulcanizates. Rubber Chemistry and Technology. 2007; 80(1):80–83. https://doi.org/10.5254/1.3548170

5. Przybytek A, Kucinska-Lipka J, Janik H. Thermoplastic elastomer filaments and their application in 3D printing. Elastomery. 2016; 20(4):32–39. https://doi.org/10.1016/B978-0-12-818311-3.00012-4

6. Lim KHA, Loo ZY, Goldie SJ, Adams JW, McMenamin PG. Use of 3D printed models in medical education: A randomized control trial comparing 3D prints versus cadaveric materials for learning external cardiac anatomy. Anatomical Sciences Education. 2016; 9(3):213–221. https://doi.org/10.1002/ase.1573

7. Tappin SW. Canine tracheal collapse. Journal of Small Animal Practice. 2016; 57(1):9–17. https://doi.org/10.1111/jsap.12436

8. Jung SY, Lee SJ Kim HY, Park HS, Wang Z, Kim HJ, Yoo JJ, Chung SM, Kim HS. 3D printed polyurethane prosthesis for partial tracheal reconstruction: a pilot animal study Biofabrication. 2016; 8(4):045015. https://doi.org/10.1088/1758-5090/8/4/045015

9. Bedoya SAO, Conceição LG, Viloria MIV, Loures FH, Valente FL, Amorim RL, Silva FF. Caracterização de colágenos tipos I e III no estroma do carcinoma de células escamosas cutâneo em cães. Arquivos Brasileiros de Medicina Veterinária e Zootecnia. 2016; 68(1):147–154. https://doi.org/10.1590/1678-4162-8484

10. Grillo HC. The history of tracheal surgery. Chest Surgery Clinic. 2003; 13(2):175–189. https://doi.org/10.1016/s1052-3359(03)00002-4

11. Zhang H, Fu W, Xu Z. Re-epithelialization: a key element in tracheal tissue engineering. Regenerative Medicine. 2015; 10(8):1005–1023. https://doi.org/10.2217/rme.15.68

12. Townsend JM, Ott LM, Salash JR, Fung KM, Easley JT, Seim HB 3rd, Johnson JK, Weatherly RA, Detamore MS. Reinforced Electrospun Polycaprolactone Nanofibers for Tracheal Repair in an In Vivo Ovine Model. Tissue Engineering. Part A. 2018; 24(17–18):1301−1308. https://doi.org/10.1089/ten.TEA.2017.0437

13. Kang Y, Wang C, Qiao Y, Gu J, Zhang H, Peijs T, Kong J, Zhang G, Shi X. Tissue-Engineered Trachea Consisting of Electrospun Patterned sc-PLA/GO-g-IL Fibrous Membranes with Antibacterial Property and 3D-Printed Skeletons with Elasticity. Biomacromolecules. 2019; 20(4):1765−1776. https://doi.org/10.1021/acs.biomac.9b00160

14. Park HS, Lee JS, Jungb H, Kim DY, Kim SW, Sultan MT, Park CH. An omentum-cultured 3D-printed artificial trachea: in vivo bioreactor. Artificial Cells, Nanomedicine, and Biotecnology. 2018; 46(3):1131–1140. https://doi.org/10.1080/21691401.2018.1533844

15. Hench LL. Biomaterials. Science. 1980; 208(4446):826–831. https://doi.org/10.1126/science.6246576

16. Anderson JM, Rodriguez A, Chang DT. Foreign body reaction to biomaterials. Seminars in Immunology. 2008; 20:86-100. https://doi.org/10.1016;j.smim.2007.11.004

17. Williams DF. On the mechanisms of biocompatibility. Biomaterials. 2008; 29(20):2941–2953. https://doi.org/10.1016/j.biomaterials.2008.04.023

18. 18. Williams DF. Biocompatibility Pathways: Biomaterials-Induced Sterile Inflammation, Mechanotransduction, and Principles of Biocompatibility Control. ACS Biomaterials Science & Engineering. 2016; 3(1): 2–35. https://doi.org/10.1021/acsbiomaterials.6b006

19. Gaissert HA, Grillo HC, Wright CD, Donahue DM, Wain JC, Mathisen DJ. Complication of benign tracheobronchial strictures by self-expanding metal stents. The Journal of Thoracic and Cardiovascular Surgery. 2003; 126(3):744–747. https://doi.org/10.1016/s0022-5223(03)00361-1

20. Delaere P, Raemdonck DV. Tracheal Replacement. Journal of Thoracic Desease. 2016; 8(2):186–196. https://doi.org/10.3978/j.issn.2072-1439.2016.01.85

21. Li D, Yin Z, Liu Y, Feng S, Liu Y, Lu F, Xu Y, Min P, Hou M, Li K, He, A, Zhang W, Liu W, Zhang Y, Zhou G, Cao Y. Regeneration of trachea graft with cartilage support, vascularization, and epithelization. Acta Biomaterialia. 2019; 89: 206-216. https://doi.org/10.1016/j.actbio.2019.03.003

22. 22. Chang JW, Park SA, Park J.K, Choi, JW, Kim YS, Shin YS, Kim CH. Tissue-Engineered Tracheal Reconstruction Using Three-Dimensionally Printed Artificial Tracheal Graft: Preliminary Report. Artificial Organs. 2014 38(6):95–105. https://doi.org/10.1111/aor.12310

23. 23. Han Y, Li X, Zhang Y, Han Y, Chang F, Ding J.. Mesenchymal Stem Cells for Regenerative Medicine. Cells. 2019; 8(8): 1-32. https://doi.org/10.3390/cells8080886

24. Mendonça RJ, Coutinho-Netto, J. Aspectos celulares da cicatrização. Anais Brasileiros de Dermatologia. 2009, 84(3):257-262. https://doi.org/10.1590/S0365-05962009000300007

25. Branski RC, Rosen CA, Verdolini K, Hebda PA. Biochemical markers associated with acute vocal fold wound healing: a rabbit model. Journal of Voice. 2005; 19(2):283–289. https://doi.org/10.1016/j.jvoice.2004.04.003

26. Shimizu T. Role of macrophage migration inhibitory factor (MIF) in the skin. Journal of Dermatological Science. 2005; 37(2):65–73. https://doi.org/10.1016/j.jdermsci.2004.08.007

27. Mendonça AC, Ferreira AS, Barbieri CH, Thomazine JA, Mazzer N. Efeitos do ultrassom pulsado de baixa intensidade sobre a cicatrização por segunda intenção de lesões cutâneas totais em ratos. 2006; Acta Orthopedic Brasileira. 2006; 14(3):152–157. https://doi.org/10.1590/S1413-78522006000300007

28. Alves A, Gritsch K, Sirieix C, Drevon-Gaillot E, Bayon Y, Clermont G, Boutrand JP, Grosgogeat. Computerized histomorphometric study of the splenic collagen polymorphism: A control-tissue for polarization microscopy. Microscopy Research and Technique. 2015; 78(10):900–907. https://doi.org/10.1002/jemt.22553

29. Varghese SS, Sarojini SB, George GB, Vinod S, Mathew P, Babu A, Sebastian J. Evaluation and Comparison of the Biopathology of Collagen and Inflammation in the Extracellular Matrix of Oral Epithelial Dysplasias and Inflammatory Fibrous Hyperplasia Using Picrosirius Red Stain and Polarising Microscopy: A Preliminary Study. Journal of Cancer Prevention. 2015; 20(4):275–80. https://doi.org/10.15430/JCP.2015.20.4.275

30. Berry DB, Sullins KE. Effects of topical application of antimicrobials and bandaging on healing and granulation tissue formation in wounds of the distal aspect of the limbs in horses. American Journal of Veterinary Research. 2003; 64(1):88–92. https://doi.org/10.2460/ajvr.2003.64.88

31. Dayan D, Hiss Y, Hirshberg A, Bubis JJ, Wolman M. Are the polarization colors of picrosirius red-stained collagen determined only by the diameter of the fibers? Histochemistry. 1989; 93(1):27–29. https://doi.org/10.1007/BF00266843

32. Morales-Nebreda LI, Rogel MR, Eisenberg JL, Hamill KJ, Soberanes S, Nigdelioglu R, Chi M, ChoT, Radigan KA, Ridge KM, Misharin AV, Woychek A, Hopkinson S, Perlman H, Mutlu GM, Pardo A, Selman M, Jones JCR, Budinger GRS. Lung-Specific Loss of α3 Laminin Worsens Bleomycin-Induced Pulmonary Fibrosis. American Journal of Respiratory Cell and Molecular Biology. 2015; 52(4):503–512. https://doi.org/10.1165/rcmb.2014-0057oc

33. Reis JGC Takiya CM; Carvalho AL; Mota RS; De-Ary-Pires B; Ary Pires-Neto M; Ary-Pires R. Myofibroblast

persistence and collagen type I accumulation in the human stenotic trachea. Head Neck. 2011; 34(9): 0–0. https://doi.org/10.1002/hed.21915

34. Jahshan F, Ammar AA, Ertracht O, Eisenbach N, Daoud A, Sela E, Atar S, Zussman E, Fichtman B, Harel A, Gruber M. Local Delivery of Mometasone Furoate from an Eluting Endotracheal Tube Reduces Airway Morbidity Following Long-Term Animal Intubation. ACS Applied Bio Materials. 2021; 4(5):4131–4139. https://doi.org/10.1021/acsabm.0c01526

35. Haykal S, Salna M, Waddell TK, Hofer SO. Advances in Tracheal Reconstruction. Plastic and Reconstructive Surgery-Global Open. 2014; 2(7):1–11. https://doi.org/10.1097/GOX.0000000000000097

36. Brand-Saberi BEM, Schafer T. Trachea: Anatomy and Physiology. Thoracic Surgery Clinics. 2014; 24(1):1–5. https://doi.org/10.1016/j.thorsurg.2013.09.004

37. García SR, Deprez M, Lebrigand K, Cavard A, Paquet A, Arguel M-J, Magnone V, Truchi M, Caballero I, Leroy S, Marquette C-H, Marcet B, Barbry P, Zaragosi, L.-E. Novel dynamics of human mucociliary differentiation revealed by single-cell RNA sequencing of nasal epithelial cultures. Development. 2019; 146:1-17. https://doi.org/10.1242/dev.177428

38. Kim WS, Chang JW, Jang WS, Seo YJ, Kang ML, Sung HJ, Kim DH, Kim JM, Park JH, Ban MJ, Na G, Shin SH, Byeon HK, Koh YW, Kim SH, Baik HK, Choi EC. Tracheal reconstruction with a free vascularized myofascial flap: preclinical investigation in a porcine model to human clinical application. Scientific Reports. 2017; 7:10022. https://doi.org/10.1038/s41598-017-10733-z

39. Arif U, Haider S, Haider A, Khan N, Alghyamah AA, Jamila N, Khan MI, Almasry WA, Kang I. Biocompatible Polymers and their Potential Biomedical Applications: A Review. Current Pharmaceutical Design. 2019; 25 (34):3608-3619. https://doi.org/10.2174/1381612825999191011105148